Analysis of Conformal Quad Band Metamaterial Absorber Design on Planar and Cylindrical Surface

Nitinkumar J. Bathani[1, *] and Jagdishkumar M. Rathod[2]

Abstract—A conformal metamaterial absorber operating at the quad band is analyzed in this paper. The proposed structure is fabricated on a 0.5 mm thick, flexible polyester dielectric substrate. The proposed structure works at the chosen frequencies 4.11 GHz, 5.37 GHz, 7.39 GHz, and 8.4 GHz with the absorptivities of 96%, 95%, 90%, and 94%, respectively. The structure has the essential novelty of miniaturization of $\lambda/146$ in the thickness, which is an exceptionally flexible material for Radar applications. Quad band excitation can also be analyzed by the iteration of the proposed structure as well as circuit analysis. The flexible polyester material is etched with silver coating for the development of the fabricated structure. The simulated results can also be associated with the measured ones from the planar as well as a cylindrical surface to realize flexibility for stealth technology. It can be accomplished by the free space measurement technique in an anechoic chamber.

1. INTRODUCTION

Metamaterial structures are recently very popular due to their artificial property including negative ε and μ. This helps the advancement of signal phase and increment of evanescent waves towards source. This structure was presented in 1968 by Veselego [1]. Ample amount of research has been carried out in the field of designing metamaterial absorbers. There is a massive demand of metamaterial absorber with flexibility in military applications, aircraft, and missile applications. So conformal substrate with a low dielectric constant is primarily used to implement low profile conformal metamaterial absorber. Wide-angle insensitivity is the major focus of absorber design, and configuration should give comparable results in cylinder with arbitrary radius or planar plane.

The property of a metamaterial structure can be optimized by the numerical arrangement, geometrical configuration of the unit cell structure which is a key parameter to control permittivity [2], permeability [2, 3], and refractive index [4, 5] of an arbitrary metamaterial structure. Landy et al. in 2008 [6] designed and experimentally verified the first metamaterial absorber at 11.48 GHz with an absorption rate of 96% and bandwidth of 4%. Subsequently, dual band [7, 8], tripleband [9, 10], quadband [11–15], multiband [16], and wideband [17] absorbers have been developed. Later on, conformal multiband absorbers have also been reported [12, 18, 19]. A conformal metamaterial absorber fabricated and measured on a planar or cylindrical surface was also reported [10, 20, 21]. All of them are important for the Radar cross section (RCS) reduction in Stealth Technology. This suggests that all the individualities of metamaterial absorber like conformality, multiband, polarization, and oblique angle independent in a single structure are potential research area.

In the current reported work, we have designed and fabricated an $8*8$ unit cell matrix on a 0.5 mm thick polyester substrate. The polyester substrate is used due to its flexibility and suitability for high frequency. Iteration of the structure with appropriate result and the fabricated structure are shown.

* Corresponding author: Nitinkumar J. Bathani (email@nitinbathani@gmail.com).
[1] Department of E. C. Engg., Government Engineering College, Modasa, Gujarat, India. [2] Department of Electronics, Birla Vishvakarma Mahavidyalaya, Vallabh Vidyanagar, Gujarat, India.

The structure absorbs four frequencies, 4.11 GHz, 5.37 GHz, 7.39 GHz, and 8.4 GHz, which works in L- and S-bands. Proposed structure measurement has been compiled in planar and cylindrical surface which enables it for any structure of radar and missiles. It has also been simulated and fabricated on the conformal polyester substrate, which makes it suitable in the wearable application, defense and satellite application. The article is in six sections. Section 2 integrates the optimized parameters of the presented unit cell design. In Section 3, iteration of the proposed structure and identical circuit parameters that specify the reason for the absorption of quad band are discussed. Section 4 comprises variations of the physical and electrical quantities of the proposed structure. Section 5 includes fabrication and cylindrical as well as planar measurement techniques for the practical result confirmation, and the conclusion is compiled in Section 6.

2. UNIT CELL DESIGN

Figure 1 illustrates a quadband conformal metamaterial absorber (QCMA), which has a quad-band structure on the top plane. This structure can be implicit on the flexible substrate material chosen as polyester with a loss tangent $(\tan \delta)$ of 0.003 and dielectric constant ε_r of 3.2. The structure is also implied on a planar and cylindrical copper sheet, which functions as ground plane of a proposed structure. A flexible copper sheet with a 1 mm height is used to develop a cylindrical ground plane. The finite element method simulated by HFSS software is used to solve this unit cell structure. To perform the idealistic situation of infinite periodicity, master and slave boundary is optimized in the unit cell at the parallel plane which can be energized by the Floquet port in the perpendicular plane. Metamaterial unit cell is designed by an $8*8$ notched circular resonator on the conformal polyester substrate material. The incremental electrical length provides excitation of a multiple band structure. The parameters after optimization technique through HFSS of the proposed arrangement for the unit cell are shown in Table 1.
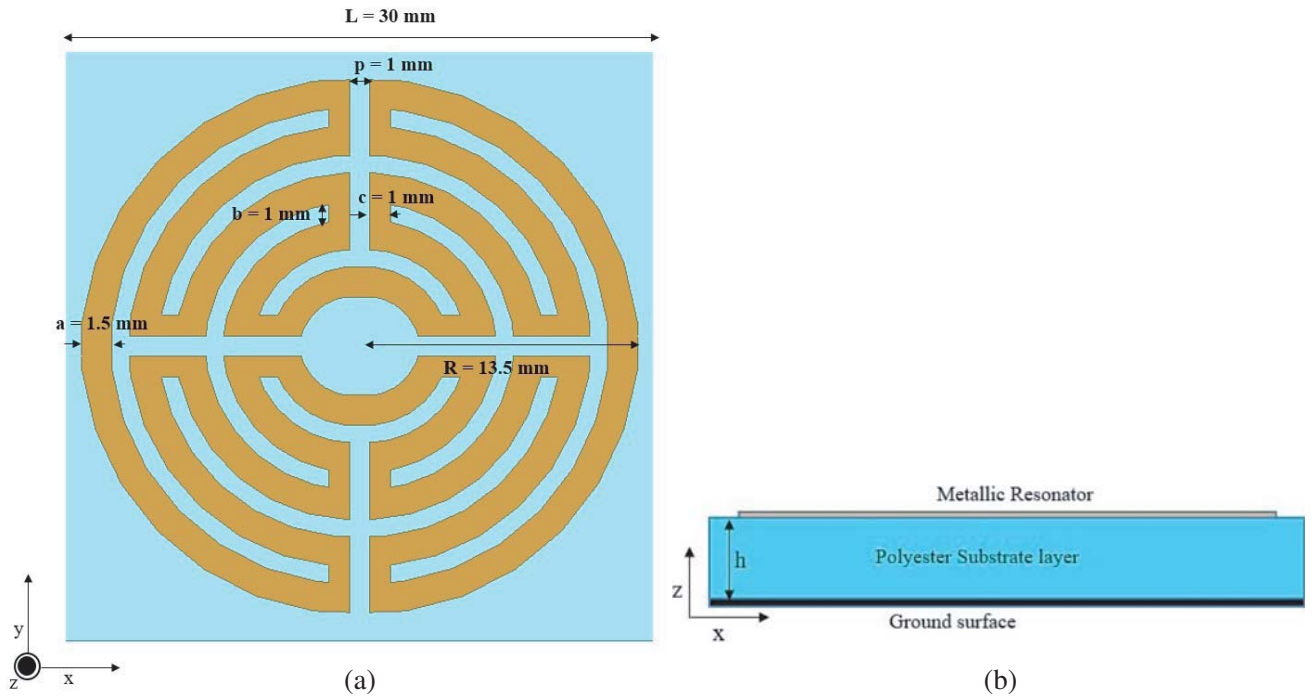

Figure 1. Simulated QCMA unit cell structure. (a) Front view. (b) Lateral view.

The chosen unit cell design size is 30 mm, which provides miniaturization to $\lambda/2.4$ at the lowest frequency. The thickness of the presented QCMA $h = 0.5$ mm, which is $\lambda/146$ miniaturized at the lowest frequency. The effect of substrate thickness on the multiband structure was reported in [22].

Table 1. Optimized parameters of proposed QCMA.

Parameters	L	R	a	b	c	p	h
Dimensions (mm)	30	13.5	1.5	1	1	1	0.5

3. ABSORPTION MECHANISM IN QUADBAND

Electrically long length structure in compact physical size because of the notched co-centric circular design is the main reason for working in multiple frequencies. Iteration of the proposed QCMA has been simulated for analysis. Fig. 2 shows the simulated design for multiple successive iterations of the proposed QCMA. The absorption rates for these iterative designs are shown in Fig. 3 which depicts the first iteration with a circular resonator excited at a single frequency of 4.7 GHz. The second iteration operates at dual-frequencies of 5.1 GHz and 6.7 GHz, while the third iteration can be excited with all three frequencies which are 4 GHz, 5.8 GHz, and 6.8 GHz. Hence, multiple iterations are the main reason for the excitement of quad-band frequency.

The identical circuit of proposed QCMA is depicted in Fig. 4(a). Circuit structure of proposed QCMA consists of a four resonator circuit having LC component with equivalent substrate characteristic
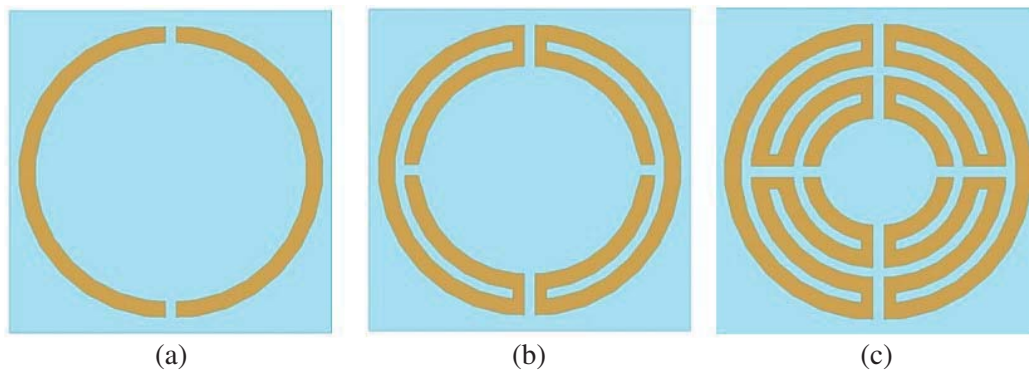

(a)   (b)   (c)

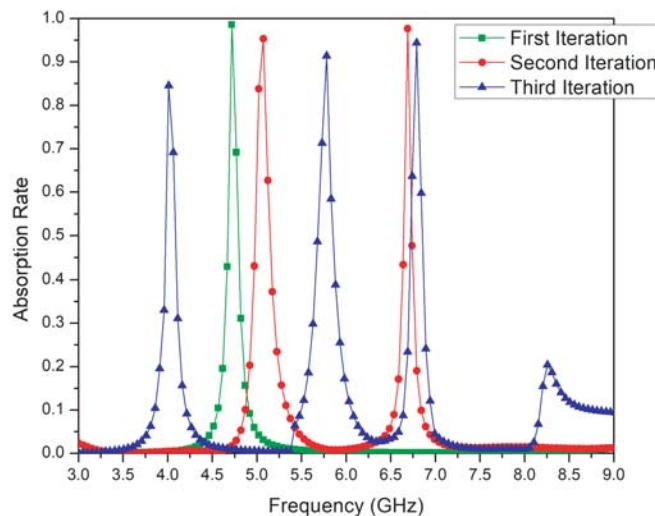**Figure 2.** (a) First iteration design. (b) Second iteration design. (c) Third iteration design.

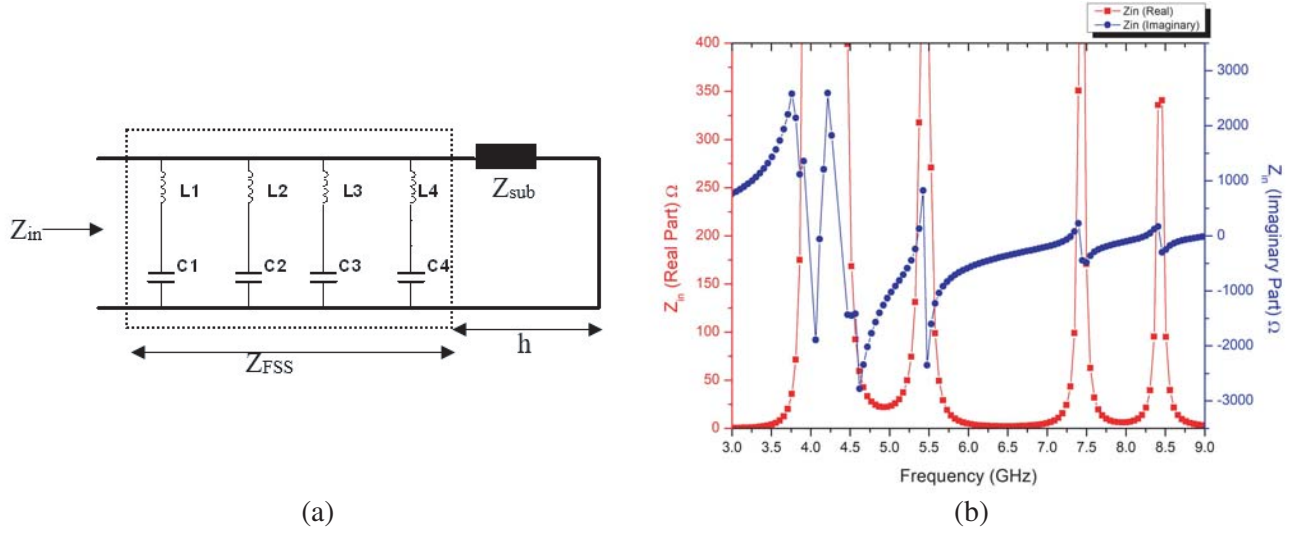**Figure 3.** Frequency vs absorption rate for successive iteration of proposed QCMA.

Figure 4. (a) Identical circuit of proposed QCMA. (b) Input impedance of Proposed QCMA.

impedance Z_{sub}, which can be identified from Equation (1)

$$Z_{sub} = \frac{Z_o}{\sqrt{\varepsilon_r}} \tan(\beta * h) \tag{1}$$

Z_o signifies the characteristics impedance, β the phase shift constant which is equal to propagation constant, and h the depth of the substrate having the value of $0.5\,\text{mm}$. The input impedance of the proposed QCMA [3] can be given by Equation (2)

$$Z_{in} = \left(\frac{1}{jwC_1} + jwL_1\right) \left\|\left(\frac{1}{jwC_2} + jwL_2\right)\right\| \left(\frac{1}{jwC_3} + jwL_3\right) \left\|\left(\frac{1}{jwC_4} + jwL_4\right)\right\| \left(\frac{Z_o}{\sqrt{\varepsilon_r}} \tan(\beta * h)\right) \tag{2}$$

The input impedance decides the value of reflection coefficient which can be identified from Equation (3)

$$\tau = \frac{Z_{in} - Z_o}{Z_{in} - Z_o} \tag{3}$$

Reflection coefficient can be minimized by matching of input resistance with the characteristics impedance. This results into minimum absorption rate which is represented in Equation (4)

$$A(f)_{QCMA} = (1 - R(f) - T(f)) * 100\% \tag{4}$$

$R(f)$ and $T(f)$ are reflection and transmission coefficients with respect to frequency which can be defined as:

$$R(f) = S_{11}(f)^2 \tag{5}$$
$$T(f) = S_{21}(f)^2 \tag{6}$$

The identical inductance and capacitance values of ring type and strip type structures can be defined from [23–25]. The proposed structure comprises concentric circles with radii $13.5\,\text{mm}$, $11\,\text{mm}$, $8.5\,\text{mm}$ and $6\,\text{mm}$ respectively with the pitch length of $1\,\text{mm}$. Inductance (L) value for this design can be inferred in Equation (7)

$$L = \mu_0 \mu_{eff} \frac{R_i}{2\pi} \ln\left(\frac{1}{\sin\dfrac{\pi\omega}{2R_i}}\right) \tag{7}$$

μ_o and μ_{eff} are permeability in free space and relative permeability. R_i is the radius of multiple concentric circles with an iteration width of $1\,\text{mm}$ of proposed QCMA. The actual width during

fabrication process may vary slightly from the width used in simulation. The effective capacitance (C) can be analyzed from [23], which is identified in Equation (8)

$$C = \varepsilon_0 \varepsilon_{eff} \frac{2\left(R_i - \frac{a}{2}\right)}{\pi} \ln\left(\frac{1}{\sin\frac{\pi\frac{b}{2}}{2\left(R_i - \frac{a}{2}\right)}}\right) \tag{8}$$

The input impedance of proposed structure at operating frequencies has an imaginary impedance of nearly zero value, and real impedance values close to intrinsic impedance which can be examined in Fig. 4(b).

Effective optimized inductance values are $L_1 = 5.78\,\text{nH}$, $L_2 = 4.28\,\text{nH}$, $L_3 = 2.87\,\text{nH}$, and $L_4 = 1.61\,\text{nH}$, whereas capacitance values are $C_1 = 0.2\,\text{pF}$, $C_2 = 0.15\,\text{pF}$, $C_3 = 0.10\,\text{pF}$, and $C_4 = 55.86\,\text{pF}$. The optimized circuit components have been simulated with ADS Software. Fig. 5 represents the return loss (dB) value with frequency through ADS Software and HFSS Software.
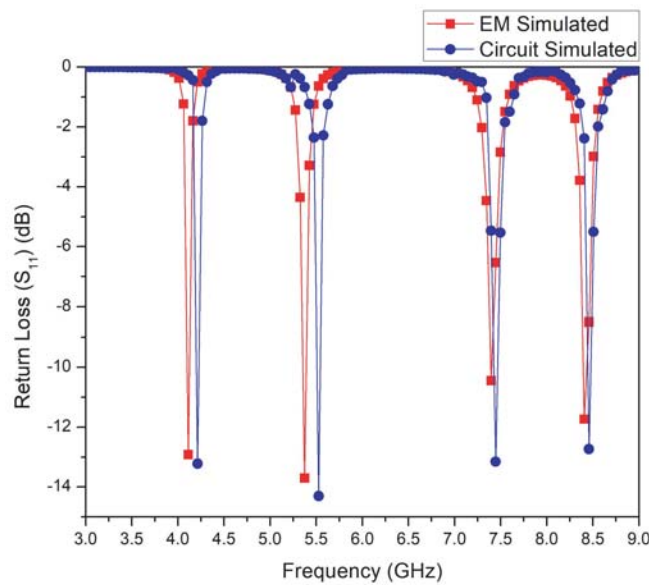

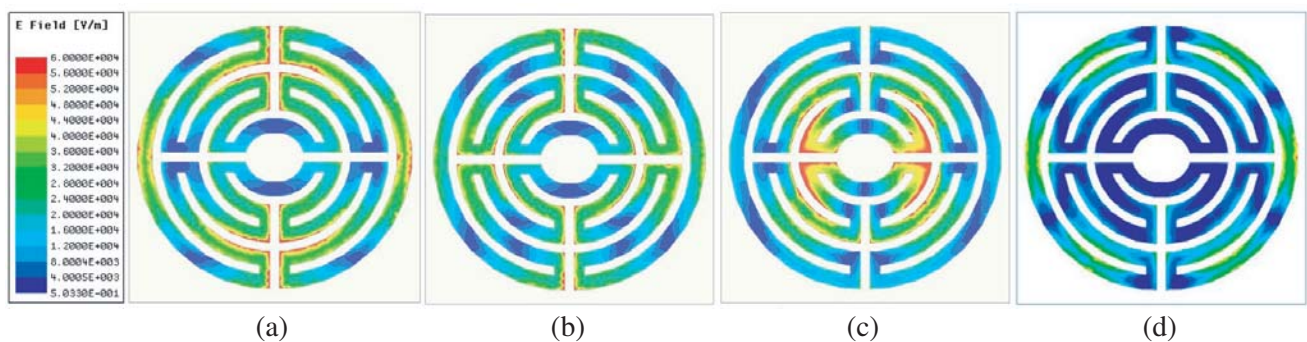**Figure 5.** Return loss of proposed QCMA in circuit and EM simulation.

Figure 6. E field distribution at the frequency (a) 4.11 GHz, (b) 5.37 GHz, (c) 7.39 GHz, (d) 8.4 GHz.
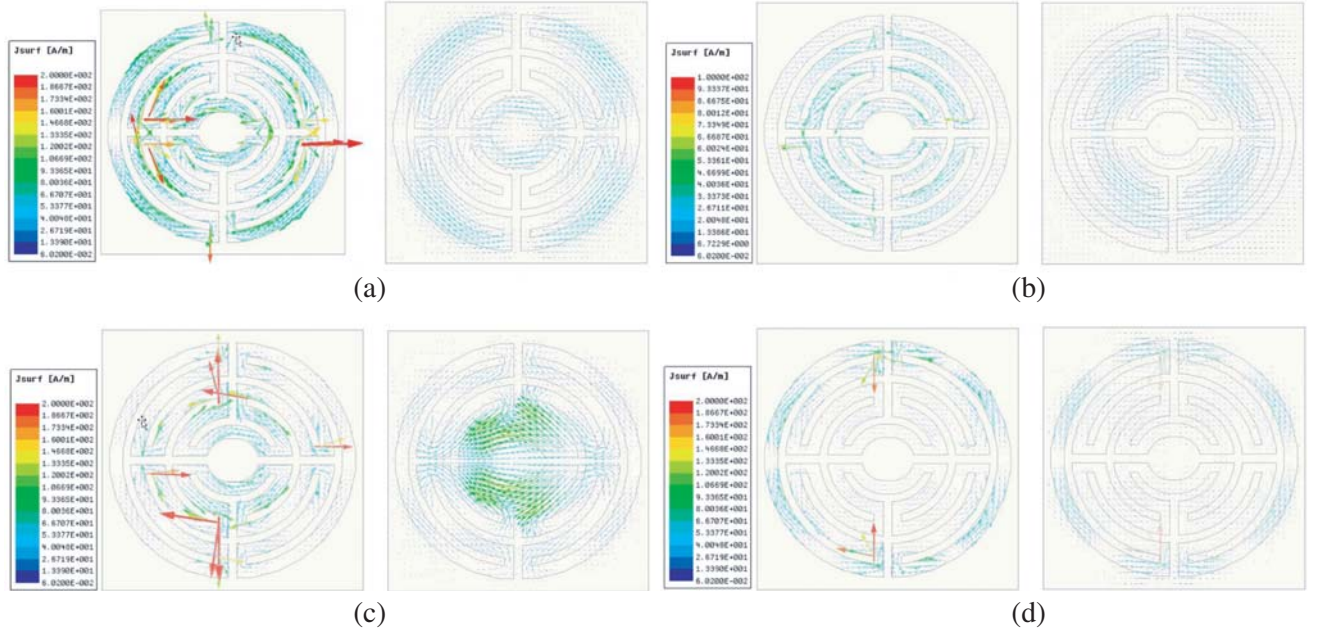
Figure 7. Front and back surface current distribution of proposed QCMA at the frequency (a) 4.11 GHz, (b) 5.37 GHz, (c) 7.39 GHz, and (d) 8.4 GHz.

The observation of electric field scattering and current density in the front and back planes gives more insight into resonance band. This has been analyzed at 4.11 GHz, 5.37 GHz, 7.39 GHz, and 8.4 GHz frequencies respectively and depicted in Fig. 6 and Fig. 7. It is observed from Fig. 6 that stronger electric field radiation is accomplished in any one of the concentric circles as per the resonant frequency, and Fig. 7 shows that current density in the top surface is anti-parallel to bottom ground plane which creates strong circulating magnetic resonance.

4. PHYSICAL AND ELECTRICAL PARAMETER VARIATION ANALYSIS

The cell design consists of large electrical length resulting in current confinement, which defines the inductance value of the proposed QCMA. The cell also consists of concentric circles with variable radius comprising of variable parasitic capacitances operating the structure at multiple resonant frequencies. The variation of parameter b in Fig. 1 affects the current confinement and parasitic capacitance of unit cell. Fig. 8(a) shows the effect of variation in the radius of concentric circles and indicates that higher operating frequency can be decreased by increasing the value of parameter b. Substrate thickness is also plays a vital role for accessing absorptivity, providing compactness and low profile property of proposed QCMA. Fig. 8(b) shows the effect of substrate thickness on the absorption rate. It shows that increase in the height of substrate does not extensively affect the resonant frequency, but for the lower value of height such as $h = 0.25$ mm, the absorptivity gets reduced to values nearly 80% at the lower resonant frequency. So 0.5 mm substrate thickness is optimally chosen for providing a low profile absorber. Fig. 9 shows the variation of the dielectric constant in the proposed QCMA. We can observe that absorption rate at any one or multiple frequencies for proposed structure lose by choosing dielectric constant except 3.2, so polyester material with a relative dielectric constant of 3.2 has been chosen for the proposed structure practically. The proposed model has been inspected at the fixed polarization angle (ϕ) for the variation in oblique angle incidence (θ). The polarization angle (ϕ) in the 0° and 90° can be evaluated for the TE and TM polarizations. The simulated absorption response for the polarization angle variation and various oblique angles is shown in Fig. 10(a). The proposed QCMA is oblique angle insensitive with a higher absorption rate up to 45° determined from Fig. 10(b).

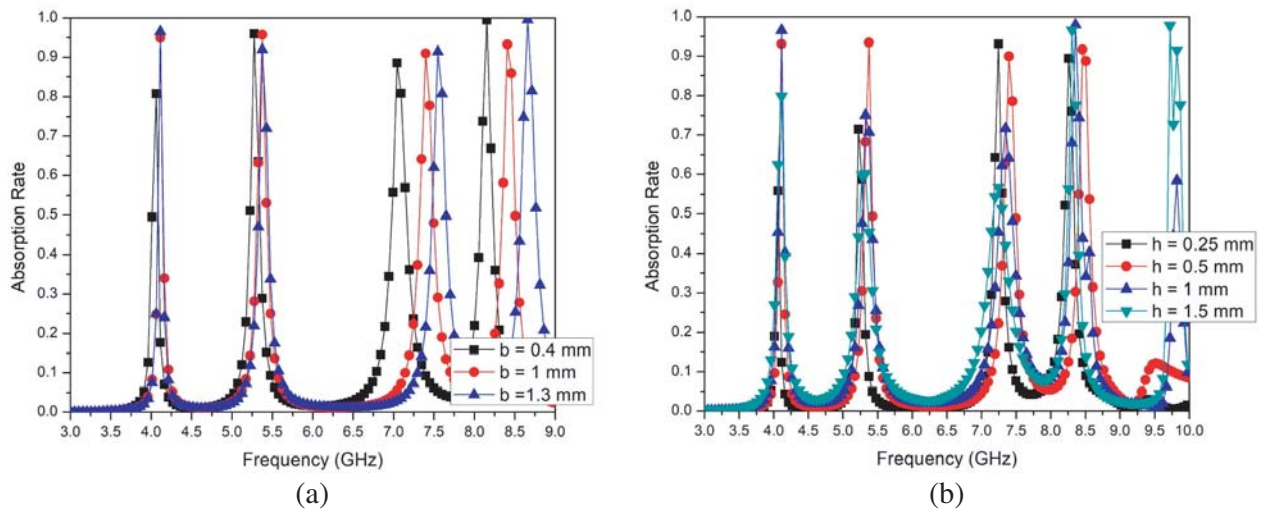Table 2 shows the comparative study of proposed structure with recently reported multi-band

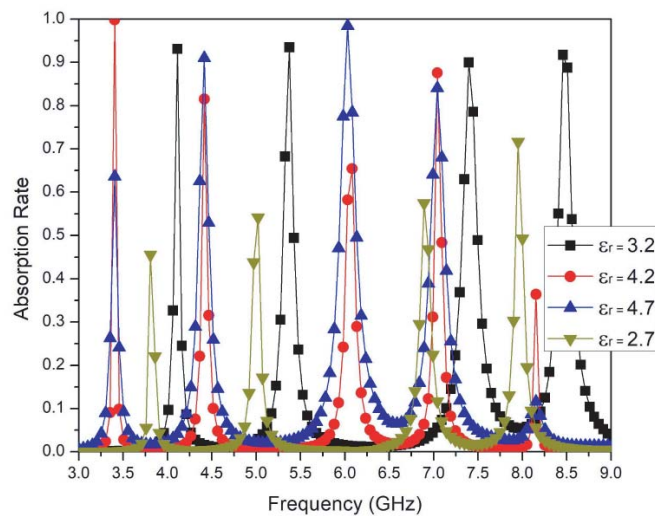**Figure 8.** Absorption rate response for variation in (a) radius of concentric circle, (b) substrate thickness.

Figure 9. Absorption rate response for variation in dielectric constant.

Table 2. Comparison between QCMA with the existing structure.

| Reference	Unit Cell Size	Substrate Thickness	Operating Frequency (GHz)	No. of Band	Conformal
H. S. Singh et al. [11]	$0.098\lambda_H$	$0.0197\lambda_H$	3.7, 6.38, 10.7, 14.27	Quad Band	No
D. Chaurasiya et al. [12]	$0.20\lambda_H$	$0.013\lambda_H$	4.1, 7.91, 10.13, 11.51	Quad Band	No
M. Agarwal et al. [13]	$0.29\lambda_H$	$0.0115\lambda_H$	4.34, 6.68, 8.58, 10.64	Quad Band	No
S. Kalraiya et al. [26]	$0.224\lambda_H$	$0.0068\lambda_H$	5.7, 7.7	Dual Band	Yes
A. K. Singh et al. [9]	$0.135\lambda_H$	$0.007\lambda_H$	2.9, 4.2, 9.6	Triple Band	Yes
G. Deng et al. [10]	$0.23\ \lambda_H$	$0.011\ \lambda_H$	8.5, 13.5, 17	Triple Band	Yes
Proposed QCMA	$0.41\lambda_H$	$0.0068\lambda_H$	4.11, 5.37, 7.39, 8.4	Quad Band	Yes
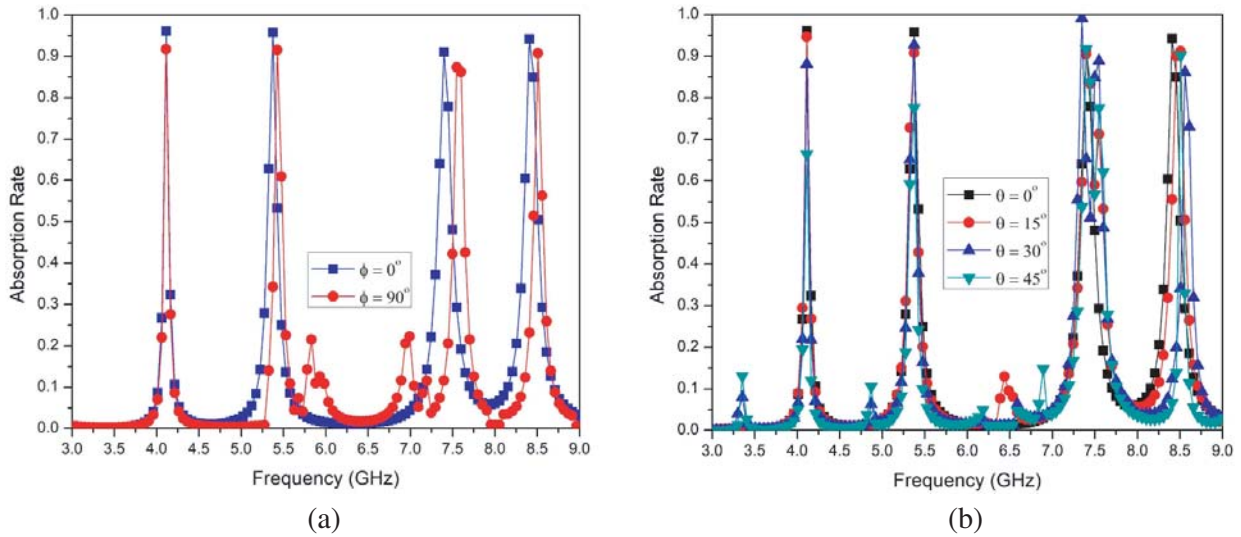
Figure 10. Absorption rate for QCMA for (a) TE and TM polarization, (b) oblique incidence.

absorbers. It indicates that the proposed structure has very ultrathin substrate providing conformal novelty working at quad band which makes it easily applicable to a higher number of band applications.

5. EXPERIMENTAL RESULTS AND DISCUSSION

A conformal structure with $8 * 8$ unit cells is fabricated in polyester material, as shown in Fig. 11, which has a total size of $24*24 \, \text{cm}^2$. The structure is engraved in a flexible copper sheet of $1 \, \text{mm}$ thickness. The absorptivity of the QCMA structure has been measured in an anechoic environment for the planar and wrapped variation of the cylindrical metallic sheet. In the measurement technique, transceiver ridged horn antenna having operating frequency band from 2 to $18 \, \text{GHz}$ can be connected to Anritsu vector
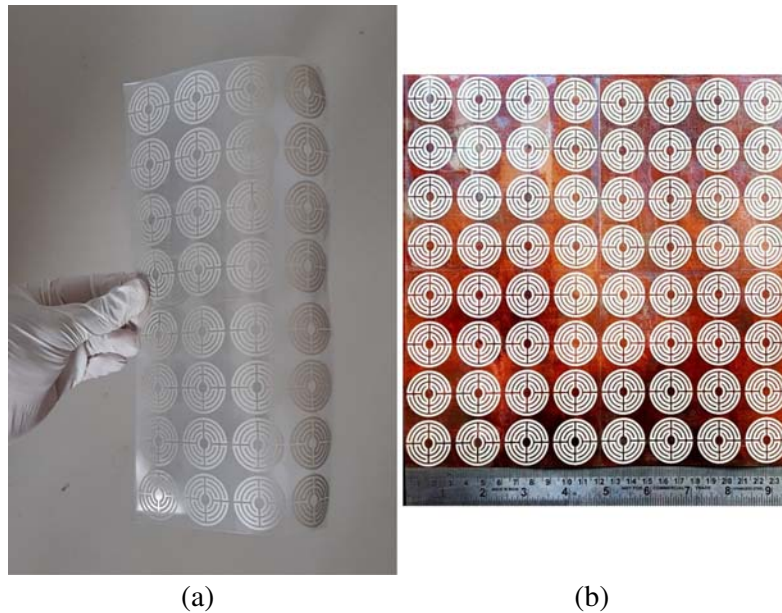

Figure 11. (a) Fabricated conformal prototype, (b) flexible QCMA engraved in copper ground plane.
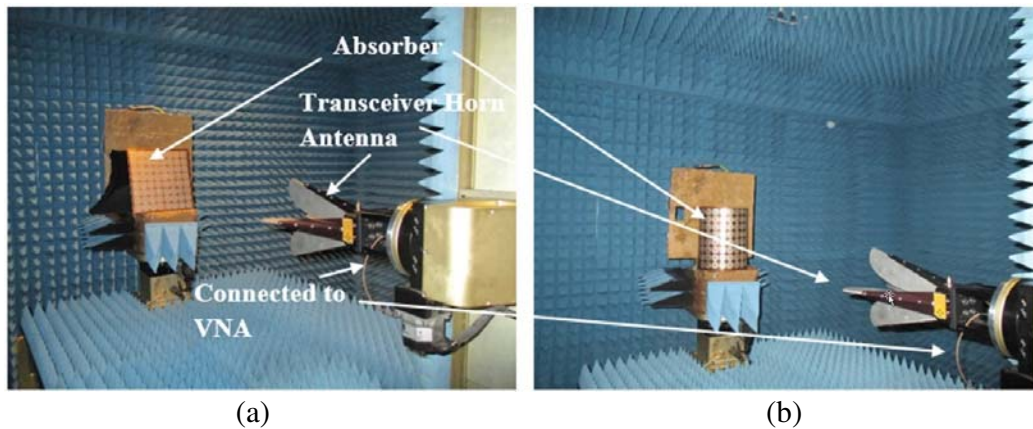
(a) (b)

Figure 12. Measurement setup of conformal absorber in (a) planar surface, (b) cylindrical surface.
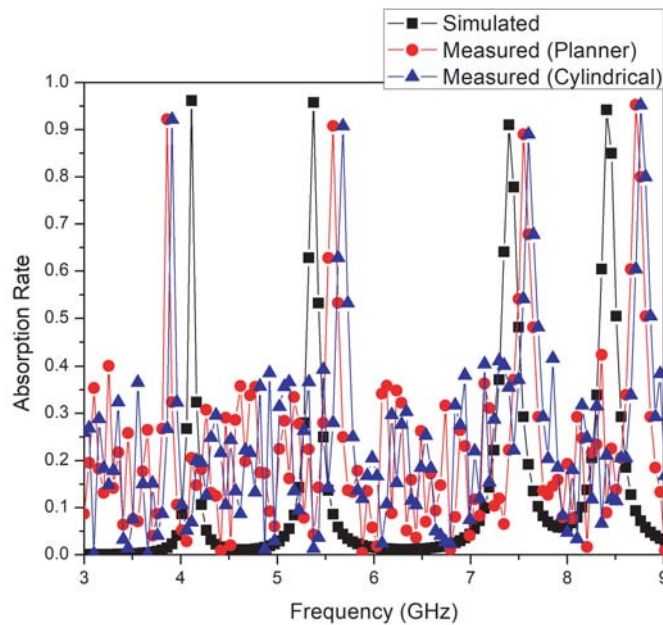

Figure 13. Comparative analysis of simulated and measured absorption rate of proposed QCMA on planar and cylindrical surface.

network analyzer MS46322B-020 with frequency band from 1 MHz to 20 GHz. The absorber under test (AUT) is positioned apart from a near field (approximately 3.5 meter) of ridged horn antenna into the anechoic chamber as shown in Fig. 12. The return loss S_{11} has been measured by comprising a copper plane in a planar and cylindrical surface with radius of 90 mm, which has been subtracted from the return loss S_{11} measured from the QCMA engraved on the copper plane at the receiver end. Fig. 13 indicates the measured result, which consists of absorptivity above 90% at 3.8 GHz, 5.6 GHz, 7.5 GHz, and 8.7 GHz, respectively. There is minimal operating frequency variation with higher absorption rate in planar and cylindrical surface. The reason for deviation of the measured response is due to lack of frequency dependent data of the dielectric constant and misalignment of structure over the copper surface.

6. CONCLUSIONS

A conformal polarization independent absorber has been introduced in this article. The novelty of the proposed QCMA exhibits a quad-band structure with ultrathin property ($\lambda_H/146$ in the thickness, where λ_H is the highest cutoff wavelength at the lowest frequency of 4.11 GHz). The proposed structure possesses absorptivity above 90% at 4.11 GHz, 5.37 GHz, 7.39 GHz and 8.4 GHz frequencies, respectively. The proposed QCMA is measured under planar as well as cylindrical surface for the practical outcome in conformal material. The simulation results of cylindrical surface with 90 mm radius and planar surface are in unison with the measurement results. The conformal behaviour of the proposed absorber has multiple applications, e.g., Radar application, wearable absorber, Stealth Technology, EMI/EMC Reduction, as well as RCS reduction application.

ACKNOWLEDGMENT

REFERENCES

1. Veselago, V. G., "The electrodynamics of substances with simultaneously negative values of ϵ and μ," *Soviet Physics Uspekhi*, Vol. 10, No. 4, 509, 1968.

2. Schurig, D., J. J. Mock, and D. R. Smith, "Electric-field-coupled resonators for negative permittivity metamaterials," *Applied Physics Letters*, Vol. 88, No. 4, 1–3, 2006, ISSN: 00036951.

3. Ziolkowski, R. W. and E. Heyman, "Wave propagation in media having negative permittivity and permeability," *Physical Review E — Statistical Physics, Plasmas, Fluids, and Related Interdisciplinary Topics*, Vol. 64, No. 5, 15, 2001, ISSN: 1063651X.

4. Smith, D. R., W. J. Padilla, D. C. Vier, S. C. Nemat-Nasser, and S. Schultz, "Composite medium with simultaneously negative permeability and permittivity," *Physical Review Letters*, Vol. 84, No. 18, 4184–4187, 2000, ISSN: 10797114.

5. Smith, D. R., J. B. Pendry, and M. C. Wiltshire, "Metamaterials and negative refractive index," *Science*, Vol. 305, No. 5685, 788–792, 2004, ISSN: 00368075.

6. Landy, N. I., S. Sajuyigbe, J. J. Mock, D. R. Smith, and W. J. Padilla, "Perfect metamaterial absorber," *Physical Review Letters*, Vol. 100, No. 20, 1–4, 2008, ISSN: 00319007.

7. S. Bhattacharyya, S. Ghosh, and K. V. Srivastava, "Equivalent circuit modeling of an ultrathin dual-band microwave metamaterial absorber," *Proc. Asia-Pac. Microw. Conference*, 1244–1266, Sendai, Japan, 2014.

8. Kaur, K. P., T. K. Upadhyaya, and M. Palandoken, "Dual-band polarization-insensitive metamaterial inspired microwave absorber for LTE-band applications," *Progress In Electromagnetics Research C*, Vol. 77, 91–100, 2017.

9. Singh, A. K., M. P. Abegaonkar, and S. K. Koul, "A triple band polarization insensitive ultrathin metamaterial absorber for S-C- and X-bands," *Progress In Electromagnetics Research M*, Vol. 77, 187–194, 2019.

10. Deng, G., K. Lv, H. Sun, J. Yang, Z. Yin, Y. Li, B. Chi, and X. Li, "An ultrathin, triple-band metamaterial absorber with wide-incident-angle stability for conformal applications at X and Ku frequency band," *Nanoscale Research Letters*, Vol. 15, No. 1, 2020, ISSN: 1556276X, [Online], Available: https://doi.org/10.1186/s11671-020-03448-0.

11. Singh, H. S., "Super compact ultrathin quad-band with wide angle stability polarization independent metamaterial absorber," *Microwave and Optical Technology Letters*, Vol. 62, No. 2, 718–725, 2020, ISSN: 10982760.

12. Chaurasiya, D., S. Ghosh, S. Bhattacharyya, A. Bhattacharya, and K. V. Srivastava, "Compact multi-band polarisation-insensitive metamaterial absorber," *IET Microwaves, Antennas and Propagation*, Vol. 10, No. 1, 94–101, 2016, ISSN: 17518733.

13. Agarwal, M., A. Behera, and M. Meshram, "Wide-angle quad-band polarisation-insensitive metamaterial absorber," *Electronics Letters*, Vol. 52, No. 5, 340–342, 2016.

14. Wang, B.-X., X. Zhai, G. Wang, W. Huang, and L. Wang, "Design of a four-band and polarizationinsensitive terahertz metamaterial absorber," *IEEE Photonics Journal*, Vol. 7, No. 1, 1–8, 2014.

15. Wang, N., J. Tong, W. Zhou, W. Jiang, J. Li, X. Dong, and S. Hu, "Novel quadruple-band microwave metamaterial absorber," *IEEE Photonics Journal*, Vol. 7, No. 1, 2015, ISSN: 19430655.

16. Jiang, H., Z. Xue, W. Li, and W. Ren, "Multiband polarisation insensitive metamaterial absorber based on circular fractal structure," *IET Microwaves, Antennas and Propagation*, Vol. 10, No. 11, 1141–1145, 2016, ISSN: 17518733.

17. M. Bağmancı, O. Akgöl, M. Özaktürk, M. Karaaslan, E. Ünal, and M. Bakır, "Polarization independent broadband metamaterial absorber for microwave applications," *International Journal of RF and Microwave Computer-Aided Engineering*, Vol. 29, No. 1, e21630, 2019.

18. Zhai, Z. C., H, Z. Li, and C. Liang, "A triple-band ultrathin metamaterial absorber with wideangle and polarization stability," *IEEE Antennas and Wireless Propagation Letters*, Vol. 14, 241–244, 2015.

19. Wu, T., Y. M. Ma, J. Chen, and L. L. Wang, "A low profile quadruple-band polarization insensitive metamaterial absorber," *Progress In Electromagnetics Research M*, Vol. 90, 69–79, 2020.

20. Sharma, S., S. K. Ghosh, and S. A. Vaibhav Srivastava Kumar, "Ultra-thin dual-band polarization insensitive conformal metamaterial absorber," *Microwave and Optical Technology Letters*, Vol. 59, No. 2, 348–353, 2017, ISSN: 10982760.

21. Libi Mol, V. A. and C. K. Aanandan, "Experimental demonstration of the performance of exible metamaterial absorber on planar and cylindrical surface," *Journal of Physics Communications*, Vol. 2, No. 1, 2018, ISSN: 23996528.

22. Kaur, K. P. and T. Upadhyaya, "Performance evaluation of wide-angle ultrathin microwave metamaterial absorber with polarization independence," *Advanced Electromagnetics*, Vol. 7, No. 4, 71–77, 2018.

23. Ebrahimi, A., S. Nirantar, W. Withayachumnankul, M. Bhaskaran, S. Sriram, S. F. Al-Sarawi, and D. Abbott, "Second-order terahertz bandpass frequency selective surface with miniaturized elements," *IEEE Transactions on Terahertz Science and Technology*, Vol. 5, No. 5, 761–769, 2015, ISSN: 2156342X.

24. Kurra, L., M. P. Abegaonkar, and S. K. Koul, "Equivalent circuit model of resonant-EBG bandstop filter," *IETE Journal of Research*, Vol. 62, No. 1, 17–26, 2016, ISSN: 0974780X.

25. Singh, A. K., M. P. Abegaonkar, and S. K. Koul, "Dual-and triple-band polarization insensitive ultrathin conformal metamaterial absorbers with wide angular stability," *IEEE Transactions on Electromagnetic Compatibility*, Vol. 61, No. 3, 878–886, 2019, ISSN: 00189375.

26. Kalraiya, S., M. Ameen, R. K. Chaudhary, and R. K. Gangwar, "Compact ultrathin conformal metamaterial dual-band absorber for curved surfaces," *International Journal of RF and Microwave Computer-Aided Engineering*, Vol. 29, No. 12, 1–9, 2019, ISSN: 1099047X.